www.s2is.org
International Journal on Smart Sensing and Intelligent Systems
ISSN 1178-5608

THE VIBRATION AND MEASUREMENT OF DRIVING MODE OF THE TWO-STAGE DECOUPLED MICRO-MACHINED GYROSCOPE

Yao Fenglin[1, 2], Gao Shiqiao[2], Zhao Jie[3], Liu Haipeng[2], Niu Shaohua[2], Jin Lei[2]
[1] Taiyuan University of Science and Technology, Shanxi, China,
[2] School of Mechatronical Engineering, Beijing Institute of Technology, Beijing, China,
[3] Department of Computer Engineering, Taiyuan University, Shanxi, China,

Emails: yfl@bit.edu.cn, gaoshq@ bit.edu.cn ,tydxcomputer@163.com,lhp@bit.edu.cn,shh@bit.edu.cn,

Abstract- This paper introduces the working principle of the two-stage decoupled micro-machined gyroscope, and establishes the vibration equation of the driving mode. By solving the differential equation, the analytical solution and the amplitude-frequency characteristics of the driving mode are obtained. By the visual measurement based on high-speed photography and the post image processing, it measures the natural frequency of the driving mode of the micro-machined gyroscope. And it measures the damping coefficient in time domain and frequency domain respectively using this method. The comparison to the theoretical solution proves that the method is effective and accurate; it will help the study for the micro-machined gyroscope vibration and provides a new way to measure MEMS.

Index terms*: decoupled, micro-machined gyroscope, driving mode, vibration, measurement.

1599

I.   INTRODUCTION

Gyroscopes have played an important role in aviation, space exploration and military applications. Until recently, high cost and large size made their use in automobiles and other consumer products prohibitive. With the advent of micro electromechanical systems (MEMS), gyroscopes and other inertial measurement devices can now be produced cheaply and in very small packages in the micro domain. An example of this are the MEMS accelerometers now used in some automobiles to detect collisions for air bag deployment [1].

The micro-machined gyroscope has tow vibration mode when it works in normal operation condition. One is the driving mode; the other is the detecting mode. The two modes has different dynamic characteristic in different driving volt and different barometric pressure[2].The two-stage decoupled gyroscope can decrease the mechanical coupling error and eliminate the identical frequency disturbing. The principle of the two-stage decoupled gyroscope is shown in Figure 1 [3].The inertial mass is supported by elastic beams consists of inner frame and outer frame, which form the movable structure [4]. When driving combs are applied by an alternating driving voltage, the whole structure is vibrating by simple harmonic vibration in X direction.
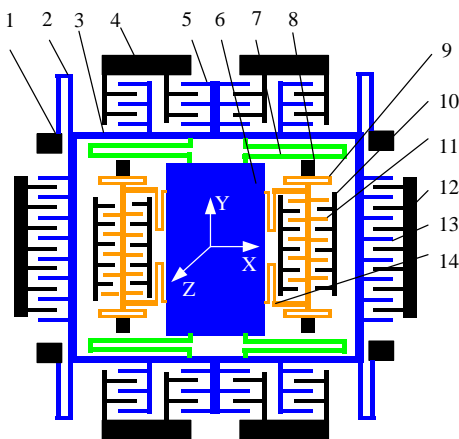

Figure 1 Configuration principle of decoupled micro gyroscope

1 Anchor point, 2 Driving bow beam, 3 Driving outer frame, 4 Fixed end of driving comb-capacitance, 5 Movable end of differential driving comb-capacitance, 6 Sensitive mass block, 7 Sensitive bow beam, 8 Anchor point, 9 Testing double bow beam, 10 Fixed end of detection capacitance, 11 Movable end of detection capacitance,12 Fixed end of driving-detection capacitance, 13 Movable end of driving-detection capacitance,14 Decoupled bow beam

When input the angular velocity of Z direction ,the inner frame which named as sensitive mass block can move in the direction of Y, will produce a displacement of Y direction because of coriolis forces. The variation of the capacitance consisting of movable and fixed combs can be measured to calculate the displacement in Y direction [5]. Because the variation of the capacitance is corresponding to angular velocity that input in Z direction, thus we can calculate angular velocity by detecting the variation of the capacitance. The movement in X direction is called driving mode, the movement in Y direction is called detecting mode [6].

In the two-stage decoupled micro gyroscope, every direction use two-stage bow beams. The bow beam can be approximately considered as have a one-dimensional degree freedom, while in the vertical direction is rigid. Despite sensitive mass block has two degrees of freedom, detecting capacitance has only one degree of freedom,it makes that micro-machined gyroscope can inhibit the mechanical coupling error under a minimal range by depending on its self-structure and solve the coupling problem of driving mode and detecting mode, which can raise the capability of the micro-machined gyroscope greatly[7-8].

II.   THE VIBRATION IN THE DRIVING MODE

For the two-stage decoupled micro-machined gyroscope, the mass of the whole driving system is m_1 .The   mass of the sensitive mass block is m_2 .The mass of the detecting system is m_3 .The stiffness of the driving bow beam in the driving direction is k_{1x} and in the detecting direction is k_{1y} .The stiffness of the sensitive bow beam in the driving direction is k_{2x} and in the detecting direction is k_{2y} .The stiffness of the decoupling bow beam in the driving is k_{3x} and in the detecting direction is k_{3y} . The stiffness of the detecting bow beam in the driving is k_{4x} and in the detecting direction is k_{4y} .When designing the structure, it make k_{1y} , k_{2x} , k_{3y} , $k_{4x} \rightarrow \infty$ which make them have one freedom in one direction and show rigid in other direction. The corresponding damping coefficients are c_{1x} , c_{2y} , c_{3x} , c_{4y} .The vibration of the driving mode is a second-order vibration system. When the exterior diving force is $F = F_0 \sin(\omega t)$,the differential equation of it is:[9]：

$$(m_1 + m_2)\ddot{x} + (c_{1x} + c_{3x})\dot{x} + (k_{1x} + k_{3x})x = F_0 \sin \omega t \qquad （1）$$

It can be simplified as：

$$m_x \ddot{x} + c_x \dot{x} + k_x x = F_e \sin \omega t \tag{2}$$

m_x is the mass of driving mode，c_x is the viscous damping,，k_x is the stiffness of the driving mode, x is the displacement of the driving mode, F_e is electrostatic driving force. And equation can change to as follow:

$$\ddot{x} + 2\xi\dot{x} + \omega_n x = \frac{F_e}{m_x} \sin \omega t \tag{3}$$

For small damping，the stationary solution of it is：

$$x = B \sin(\omega t - \varphi) \tag{4}$$

B is the amplitude of the stationary solution

$$B = \frac{B_0}{\sqrt{(1-\lambda^2)^2 + (2\xi\lambda)^2}} \tag{5}$$

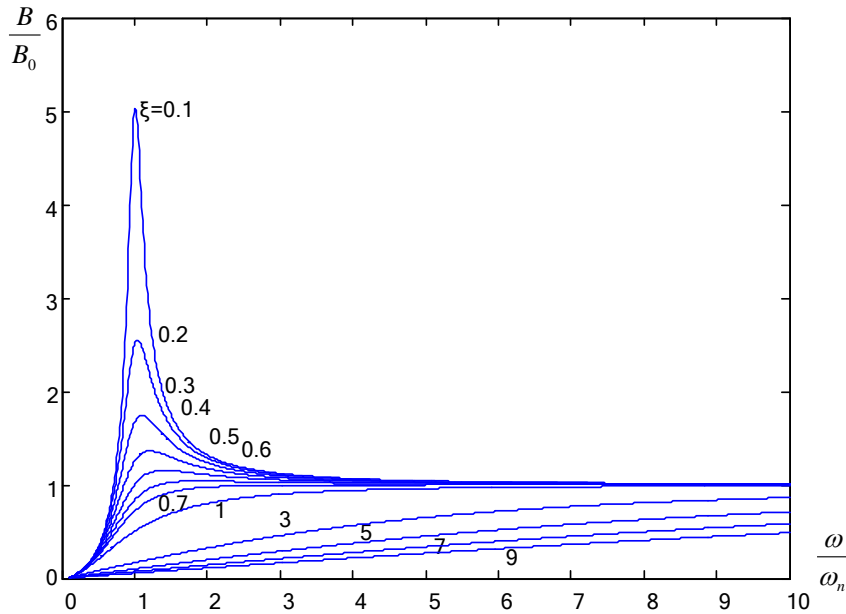The displacement of the system under different damping ratio shown in Figure 2

Figure 2 Vibration frequency and amplitude in different damping ratio

Under small damping，$\xi \ll 1, \sqrt{1-2\xi^2} \approx 1$ which means $\lambda \approx 1$,it is believed that the frequency of the exciting force nearly equal to the frequency of the natural frequency when resonance

happened. And the resonance frequency can be regarded as $\omega = \omega_n$. The vibration of the micro-machined gyroscope is a small damping vibration.

III. THE RESONANCE METHOD AND SETUP OF HIGH SPEED PHOTOGRAPHY

It is easy to see from equation 4; measure the displacement-frequency diagram can get the natural frequency. In measure the natural frequency of the common mechanical system, the vibration generator will be used, alternating the exciting frequency and measure the corresponding response with sensors. When the amplitude reaches the maximum, the vibration frequency is the resonance frequency. And the resonance equals to the natural frequency [10].But for micro-machined gyroscope, the vibration generator is impossible to act on the microstructure. The frequency sweep method is used. A digital image processing is used to detecting the amplitude variations which shows in Figure 3[11~12]。
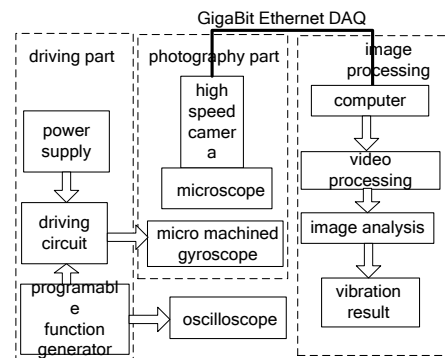

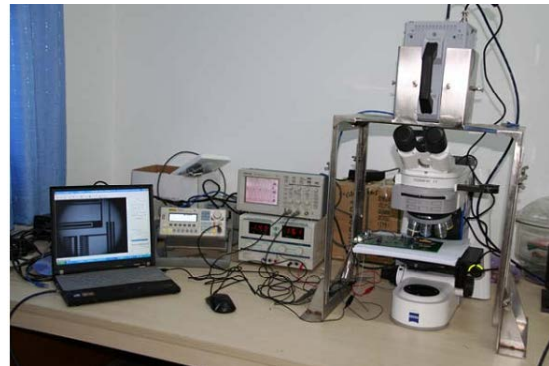Figure 3 Architecture of the system   Figure 4 Picture of image method

First, the micro gyroscope is droved to vibrating by applied AC plus DC. The driving frequency is sweeping which generated by a programmable signal generator with the frequency alternating from 3500 Hz to 5500 Hz continuously. Second, the ZEISS Image2 microscope is used in the test. Third, design value of gyroscope's natural frequency is close to 5000 Hz. Here is PHOTRON SA4 high speed camera, the sampling frequency is 30000 Hz [13].The video photographed by high speed camera is transmitted into computer by a giga Ethernet data line.

The detection system software is programmed based on MATLAB GUI. Due to the high acquisition speed of high-speed photography is up to 40,000 frame / sec, the image processing cannot handle such a huge data in real-time. The image processing belongs to post processing. The function of the processing is shown as Figure 5.
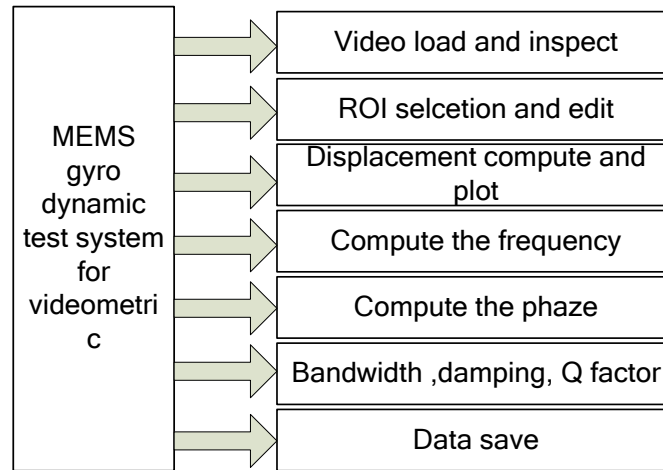
MEMS gyro dynamic test system for videometric	→	Video load and inspect
	→	ROI selcetion and edit
	→	Displacement compute and plot
	→	Compute the frequency
	→	Compute the phaze
	→	Bandwidth ,damping, Q factor
	→	Data save

Figure 5 Block diagram of software function

IV.   KEY ALGORITHM OF VIBRATION TEST BASED ON HIGH SPEED PHOTOGRAPHY

To measure the vibration of the movable part of the video image is tracking the moving target in sequential images. Target tracking must relate the image matching. The most common used image matching methods are least-square optimization matching, Mean Shift that based on the histogram matching and SURF matching that based on the feature point. Here we introduce a simple and effective method to measure the vibration in a video in MEMS [14~16].

a. Otsu threshold segmentation and geometric invariant moments method

The image processing system import the video files that shoot by the high speed camera.Then filtering and format transforming for each image in the video and image segmentation will be done. Nobuyuki Otsu proposed a threshold-based segmentation algorithm. It is an adaptive threshold determining method, also known as Otsu method[17]. It divided the image into background and target. More difference of the variance between the background and the target, more difference between the two parts which constitute the image. Either the background classified as the target or the target classified as the background will decrease the variance. Otsu method means the probability of misclassification will be minimum theoretically. The most common way of Otsu is using the maximum variance as optimum threshold between target and background of an image to segment image dynamically. In most cases，Otsu method

makes reasonable segment result. It makes pretty well result especially for the image has two peaks in the gray histogram show as Figure 6(b).

$$T^* = Arg \quad \max[w_0(\mu_0 - \mu)^2 + w_1(\mu_1 - \mu)^2] \qquad 0 \leq T \leq L \qquad (6)$$

T is the threshold, L is the maximum threshold can be used in a image. Usually, T is the gray level in an image. For a 8 bit image, L is $2^8 - 1 = 255$. w_0 and μ_0 is the percentage and average gray level of the background of the image respectively. w_1 and μ_1 is the percentage and average gray level of the target of the image respectively. μ is the average gray level of the whole image. Make T gets the maximum, and the image will segment well.

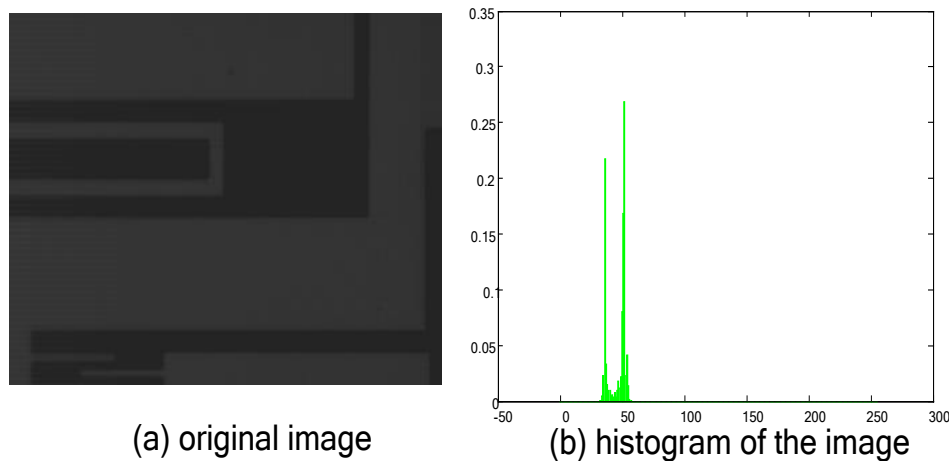(a) original image   (b) histogram of the image

Figure 6 Image and the histogram

On the other hand, after the micro gyroscope is driving, it will vibrate in high frequency. The images include the moving part and stationary part [18]. Generally, the movement can be detected by the threshold in frame difference (TIFD)[19].It use the strong dependence in the video sequences and filter on the result to detect the moving object in a video. For simplify the computation and save the computer memory, we use ROI (Region of Interest) to deal with the high speed photography. That means to process only in an interesting region. It shows the region selection near the driving beam of the micro gyroscope in Figure 7.It has higher amplitude and bigger area than others easy to detecting.
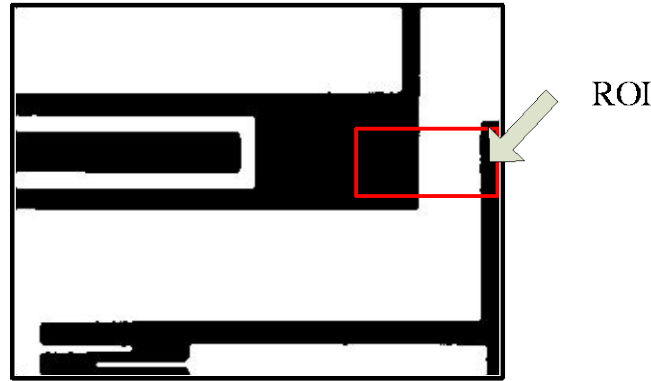
Figure 7 ROI region

Using threshold segmentation and binary image transformation can get the outline of the image. But the edge of the image is not so accurate. Although the ROI looks symmetrically, allow for the non-uniform illumination, it make the two edges are not symmetrical to their real symmetry axis in the image. Otsu method is an overall threshold of whole image. It works not so well for the local image which shows in Figure 8.So the edges after Otsu segmentation and binary transformation cannot be used as measure reference. The interval of high speed photography is so tiny. The object moving and the non-uniform of the illumination are both small in the video. Take the manufacture of the MEMS structure into account, the differential method to get edge detecting may cause errors.
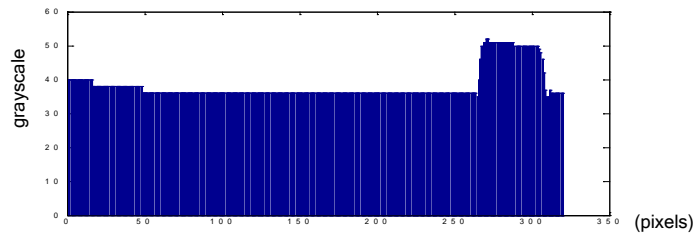
a)grayscale of the whole image
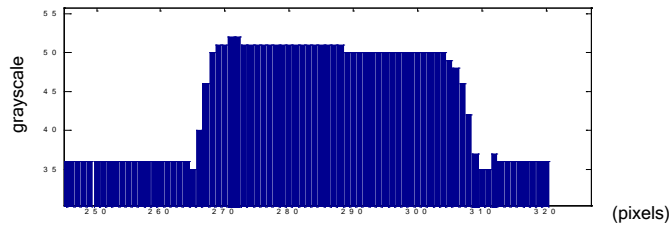
b) distribution of the local image
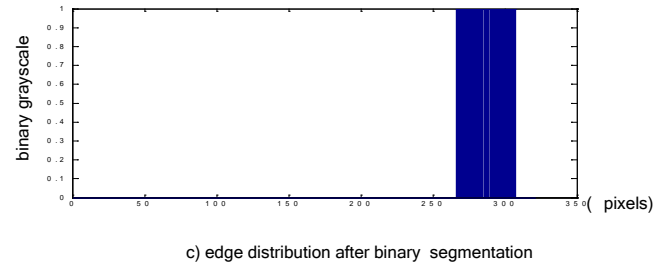
c) edge distribution after binary segmentation

Figure 8 Grayscale of Image and processing

However, the geometric characteristic of ROI in image processing can accomplish the measurement. Using the moments of the ROI image to determine the image displacement is a reasonable method.

The moments of image if suggest by Hu[20]. The $(p+q)$ order moment of image $f(x,y)$ is defined as below:

$$M_{pq} = \iint x^p y^q f(x,y)dxdy \qquad (p,q=0,1,......\infty) \qquad （7）$$

The moments of image represent the characteristics of the image and also called as geometric moments. Some of the moments possess the rotation, translation, dimension invariant and called as invariant moment. In image processing, geometric invariant moments can be used as important characteristics to present an object. And according to this, the image can be classified by the geometric invariant moments.

Moments are used to reflect the distribution of random variable in the statistics. In mechanics, it is used to describe the mass distribution in space. For the same reason, if the gray of the image is regard as a function of two-dimension or three-dimension density distribution, the moment method can be used to image analysis and feature extraction.

The most commonly used is the zero order moment that presents the "mass" of the image. It is shown as follow.

$$M_{00} = \iint f(x,y)dxdy \qquad （8）$$

The first order moment (M_{10}, M_{01}) can be used to determine the image "centroid" (X_c, Y_c).

$$M_{10} = \iint x \cdot f(x,y)dxdy \qquad （9）$$

$$M_{01} = \iint y \cdot f(x,y)dxdy \qquad （10）$$

$$X_c = \frac{M_{10}}{M_{00}} \qquad (11)$$

$$Y_c = \frac{M_{01}}{M_{00}} \qquad (12)$$

Due to the similarity of the edge sequential images in the high speed photograph video, the distribution of the edge is same. We measure the vibration of the micro gyroscope in test. So using the centroid method to detect the vibration is more reliable than using an edge detection method.

b. Algorithm implementation

The algorithm handles the nonhomogeneity on the edge of the image, eliminates the noise well and extracts the vibration accurately. In the ROI, the algorithm explains as below.

1) Select the vibration region: it is for make difference between the vibrating region and stationary region in the image for the subsequent computation. Otsu method is used for the minimum variance in black and white class which can convert a grayscale image into binary image. s is the grayscale of the pixel. The grayscale of the pixel of the vibration region convert to 1, and the grayscale of the pixel of the still region convert to 0.It is show in Figure 9

If $s > threshhold$, then $g(x, y) = 1$;Else $s < threshhold$, then $g(x, y) = 0$。

(a) original image   (b) binary image after threshold
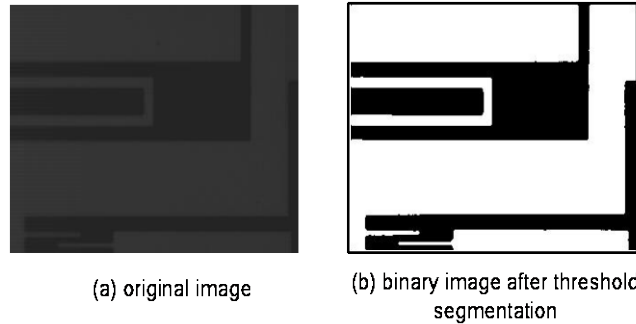   segmentation

Figure 9 Grayscale image and binary image

2）Compute the centroid of the vibration region in ROI: Calculate the number (N) all pixels whose grayscale convert to 1 in the image and extract the coordinate's (x_i, y_i).The centroid of the vibrating regions show as Eq. 13

$$\overline{x} = \frac{\sum_{i=0}^{N} x_i}{N}, \overline{y} = \frac{\sum_{i=0}^{N} y_i}{N} \qquad (13)$$

According to the centric coordinates, the vibration curve can be extract. However, the transform of the curve is different with the vibration region positioned in different ROI. Theoretically, the vibration region has two situations. One is the vibration region contained in the ROI, the other is partly contained. For the former, the centric coordinate can reflect the vibration exactly. But for the latter, the centric coordinate must do some transform to reflect the actually vibration.

3) Compute the amplitude of the micro-gyroscope. Restricted by the man-induced error and the installing condition, the vibrating region cannot insure vibrating horizontally or vertically. So relationship of the amplitude and the centric coordinate is not simple doubled. Therefore, it is possible that the gyroscope vibrates integral multiple.The sampling of the sequential image can be average. The sequential image has M frame images. The centric coordinate of every image is $(\overline{x_j}, \overline{y_j})$.The centric coordinate of the equilibrium position is $(\overline{\overline{x}}, \overline{\overline{y}})$。 The algorithm is shown as Eq. (14).

$$\overline{\overline{x}} = \frac{\sum_{j=0}^{M} \overline{x}_j}{M}, \overline{\overline{y}} = \frac{\sum_{j=0}^{M} \overline{y}_j}{M} \qquad （14）$$

For the frame j， the actually vibration can be calculated as below.

$$s_j = 2\sqrt{\left(\overline{x}_j - \overline{\overline{x}}\right)^2 - \left(\overline{y}_j - \overline{\overline{y}}\right)^2} \qquad （15）$$

4）Acquire vibration signal continuously. One image only can extract one amplitude once. Vibration curve needs a sequential image that makes the high speed camera shoot continuously. At the same time, the measurement detects the dynamic characteristics of the micro-gyroscope which makes the sampling frequency greater 10 times than the vibration frequency.
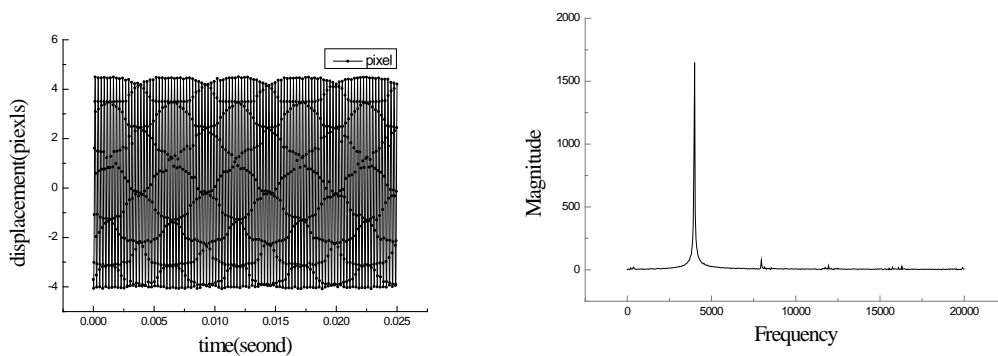

Figure 10 time-displacement and frequency-magnitude

Through digital image processing, the vibration video convert into vibration curve as shown in Figure 10 .1000 points in a time-displacement (pixel) curve that the micro gyroscope is driven in a set frequency. The frequency-magnitude shows that it is quite in line with the theoretical solution of the differential equation shown in Figure 2.

V.   NATURAL FREQUENCY OF THE MICRO GYROSCOPE

Because of the natural frequency of the micro gyroscope is sensitive to the circumstance such as temperature and atmosphere pressure etc. So the natural frequency is different greatly from the design value. Here we introduce a method to measure the natural frequency using the high speed photography and digital image processing system.

It is well know that when the driving frequency is equal to the natural frequency, the driving mode resonance occurs [21]. The diving mode has maximum amplitude and the frequency is called resonant frequency [22].We drove the micro gyroscope to vibrate under a frequency alternating from 3500 Hz to 5500 Hz continuously in just 0.6 second. This will ensure that the natural frequency will be swept. The displacement of the driving beam is shown in Figure 11.By fast Fourier transform (FFT) and filtering processing on the data listed in Figure 11, the micro gyroscope's amplitude-frequency characteristic curve is shown in Figure 12. It is concluded that micro gyroscope's resonant frequency is 3985.3 Hz.
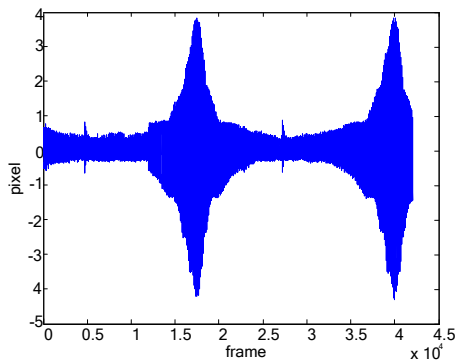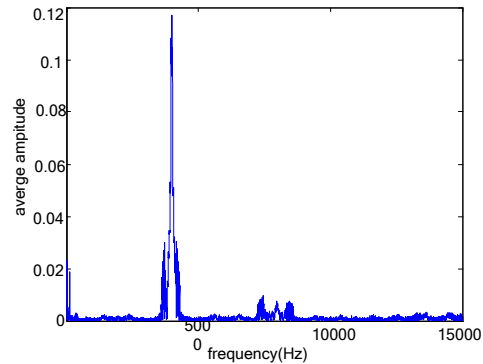

Figure 11 Sweep frequencies of drive mode   Figure 12 Average amplitude-frequency
characteristics of driving mode

IV. DAMPING MEASUREMENT

a.Free vibration method（time domain）[23]

For micro gyroscope, because of little air packaged in it, there is squeeze-film damping, slide film damping in it. And consider the micro size effect of the MEMS structure, the calculation of the damping of the microfluid is become significantly difficult and difficult to fix. The most common method is free vibration method and half power point method.

The free vibration method uses the curve of vibration with attenuation to calculate the damping. Under small damping, that is $n < \omega_n$,the solution of the vibration of the system is:

$$x = Ae^{-nt} \sin(\sqrt{\omega_n^2 - n^2}t + \alpha)$$

（16）

In equation 16, the amplitude of vibration Ae^{-nt} attenuate with time t continuously shows in Figure 14.
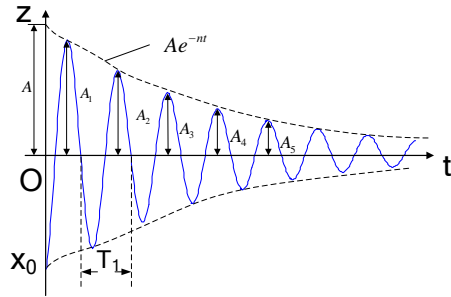

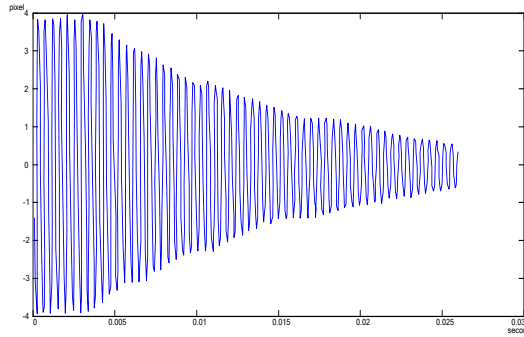Figure 13 Vibration attenuation   Figure 14 Vibration attenuation

T_1 is the cycle of the vibration attenuation and it is:

$$T_1 = \frac{2\pi}{\sqrt{\omega_n^2 - n^2}} = \frac{2\pi}{\omega_n\sqrt{1-\xi^2}}$$

（17）

Amplitude attenuation

$$\eta = \frac{A_i}{A_{i+1}} = \frac{Ae^{-nt_i}}{Ae^{-n(t_i+T_1)}} = e^{nT_1}$$

（18）

Logarithmic amplitude attenuation

$$\delta = \ln\eta = \ln\frac{A_i}{A_{i+1}} = nT_1$$

（19）

Substitute $\xi = \dfrac{n}{\omega_n}$ and $T_1 = \dfrac{2\pi}{\omega_n\sqrt{1-\xi^2}}$ in to equation 19,

$$\delta = \frac{2\pi\xi}{\sqrt{1-\xi^2}} \qquad (20)$$

Under small damping, i.e. $\xi \ll 1$ 时，$\delta \approx 2\pi\xi$，then

$$\xi \approx \frac{\delta}{2\pi} = \frac{1}{2\pi}\ln\frac{A_i}{A_{i+1}} \qquad (21)$$

When the amplitude attenuation η is small, that means the damping of the system is small. It is often used two wave crests far away to calculate the damping，and increase the precision. If use the two amplitude of i th and $(i+N)$ th wave crest ,i.e. A_i and A_{i+N} respectively, then

$$\delta = \frac{1}{N}\ln\frac{A_i}{A_{i+N}} \qquad (22)$$

The test uses the video that micro gyroscope driving mode vibrating under normal driving (the driving frequency is natural frequency: 3980Hz) and then transforms to the state of no driving volt. The vibration system attenuates to the free vibration quickly.

Measuring the amplitudes of Figure 13, data get as follow. The start point (0.01329, 3.712)，the second wave crest point(0.01341, -3.643)；the 9th wave crest point(0.01429, 3.201)，the 10th wave crest point (0.01442, -3.111)；the 89th wave crest point (0.02432, 0.7019)，the 90th wave crest point (0.02445, -0.6683).

Using equation 18 and the initial part of the vibration attenuation (point 1, 2, 9, 10), the logarithmic amplitude attenuation can be calculated as $\delta = 152.51$.In the similar way, using the initial part and the end part data (point 9, 10, 89, 90), the logarithmic amplitude attenuation can be calculated as $\delta = 152.34$.Two amplitude attenuation δ are almost the same. It reveals that the two calculations are accurate to test the amplitude attenuation curve. Furthermore, according to equation 21, the damping coefficient is calculated as 0.006097.

b. Half power point method（frequency domain）

The dynamic magnification factor of single degree freedom system is $\beta = \frac{B}{B_0} = \frac{1}{\sqrt{(1-\lambda^2)^2 - (2\xi\lambda)^2}}$, the frequency response curve of it is shown in Figure 15.

In small damping，$\lambda \ll 1$，peak value is approximate $\beta_{max} = \frac{1}{2\xi}$;
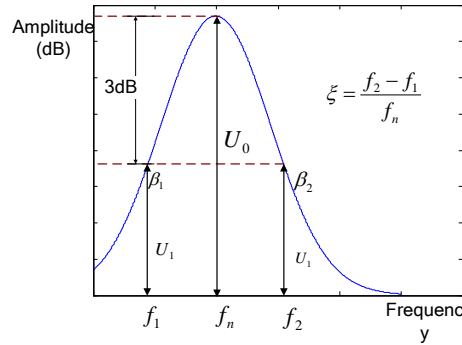
Figure 15 Sketch of half power point method calculate damping

When $\beta = \dfrac{\beta_{max}}{\sqrt{2}} = \dfrac{1}{\sqrt{2}} \cdot \dfrac{1}{2\xi}$, there are two points in the amplitude-frequency characteristic curve

β_1 and β_2 . β_1 and β_2 are called half power point. β_1 and β_2 math frequency

ratio $\lambda_1 = \dfrac{\omega_1}{\omega_n}$ and $\lambda_2 = \dfrac{\omega_2}{\omega_n}$ respectively. The corresponding frequency is ω_1 and ω_2 .Then

$\xi = \dfrac{\omega_2 - \omega_1}{2\omega_n} = \dfrac{f_2 - f_1}{2f_n}$ .The test uses the video that micro gyroscope driving mode vibrating under

normal driving (the driving frequency is natural frequency: 3980Hz). The travel-time curve is
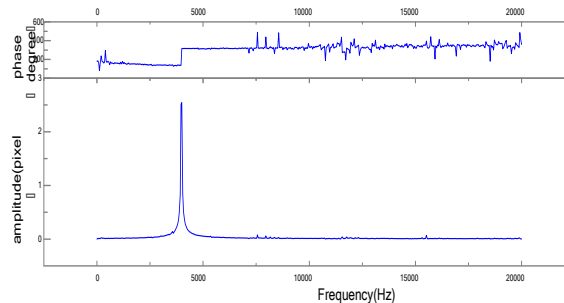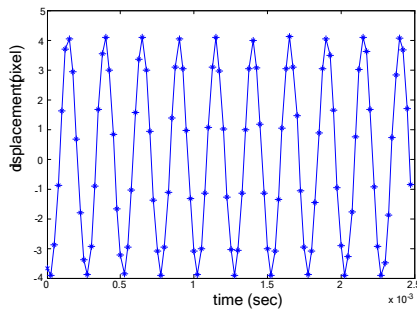
shown in Figure 16.

Figure 16 Travel-time curve under normal driving   Figure 17 Frequency characteristics under

normal driving

For the continuous signal and stable vibration, FFT also can calculate the amplitude-frequency

characteristic curve which is shown in Figure 17.Using half power point method on the first

resonance hump, the relative damping ratio ξ can be calculated.

Compare half point power method with free vibration method in measuring the damping

coefficient, the difference is 0.000063 and less than 1%.The two completely different method

using time domain and frequency to measure the damping has so close result. It effectively proves that the two methods are correct, effective.

VI.   CONCLUSION

Using the high speed photograph, the natural frequency of the driving mode of two-stage decoupled gyroscope is measured and tested. The algorithm and implementation is detailed described.And using two different methods, the damping of the vibration is tested. Using the digital image processing to measure and test the vibration of the micro gyroscope, it is a non-contact measurement and has certain feasibility. Although it is used only on the vibration of driving mode and has particular difficult to use it on the detecting mode, it provides a novel method for the research of dynamic characteristics of microstructure of MEMS.

REFERENCES

[1] Zhu Zhen,Al-Mamun, A.; Naing, "Control-centric simulator for mechatronics design case study: gyroscopically stabilized single wheel robot", International Journal on Smart Sensing and Intelligent Systems, Vol.2, no.2, 2009,pp.537-546.

[2] CHI Xiaozhu, Cui Jian, YAN Guizhen. "Electrical method to measure the dynamic behaviour of a MEMS gyroscope sensor", Chinese Journal of Sensors and Actuators, Vol.21, no.4, 2008, pp.559-562.

[3] CHEN Weiping, CHEN Hong, GUO Yugang et al. "Doubly Decoupling Mechanism of a Fully Symmetrical Micromachined Gyroscope", Nanotechnology and Precision Engineering, Vol.7, no.3, 2009, pp.239-244.

[4] GEIGER W, BUTT W, GAIBER A, et al. "Decoupled micro gyros and the design principle DAVED", Sensors and Actuators, Vol. A, no.95, 2002, pp. 235-245.

[5] JIAN Ming, YANG Fu-jun, Dong E-liang et al. "Analysis of mechanical characteristics in the double linear vibratory gyroscope using high speed photography", Optics and Precision Engineering, Vol.14, no.1, 2006, pp.121-126.

[6] Gao Shiqiao, liu Haipeng．"MEMS force"．Beijing China：Defense press，pp. 160-168, 2008．

[7] Lin Ye, Mo Jin-qiu．" Design and simulation of a new double decoupled micro machined gyroscope", Computer Simulation, Vol.22, no.4, 2005, pp. 20-24.

[8] Chakraborty, Subha．"Development and characterization of surface micro-machined mems based varactor", Vol.3, no.1, 2010, pp. 94-107.

[9] Wen Bangchun, Liu Shuyin, Chen Zhaobo et al. "Theory of mechanical vibration and its applications"．Beijing：Higher education press,2009,pp. 16-62.

[10] Yin Xiangchao．" Theory of vibration and Testing technology", Xuzhou：China University of mining and technology press, 2007, pp. 220-224.

[11]Yao Fenglin, Gao Shiqiao. "Dynamic test of vibration for micro machined gyroscope based on high speed photography". Optics and Precision Engineering, Vol.20, no.1, 2012, pp.165-171.

[12]Jin Cuiyun, Li Dachao, et al. . "Measurement Technique of In-plane Motion for MEMS Based on Machine Micro-vision", Chinese journal of scientific instrument, Vol.26, no.8, 2005, pp. 772-774

[13]Jiang Ming, He Xiaoyuan. "Optical testing of dynamic characteristic of vibrating wheel micromechanical gyroscope", Optics and Precision Engineering, Vol.16, no. 2, 2008, pp. 295-299.

[14]Lee, Sang Rok. "A coarse-to-fine approach for remote-sensing image registration based on a local method" ,international Journal on Smart Sensing and Intelligent Systems, Vol. 3, no.4,2010, pp. 690-702.

[15] Rimminen, H. "Positioning accuracy and multi-target separation with a human tracking system using near field imaging", International Journal on Smart Sensing and Intelligent Systems, Vol. 2, no.1, 2009, pp. 156-75.

[16] Jayakumar, T. "Sensors for monitoring components, systems and processes", International Journal on Smart Sensing and Intelligent Systems, Vol. 3, no.1, 2010, pp. 61-74

[17] Otsu, N., "A threshold selection method from gray-level histograms", IEEE Transactions on Systems, Man, and Cybernetics Vol. 9, no.1, 1979, pp. 62-66

[18]Yao Fenglin, Gao Shiqiao. "Vibration test of micro machined gyroscope based on high speed photography and SURF", Journal of Beijing Institute of Technology，Vol.21, no.2, 2012, pp.179-184.

[19] Wei juanli, ,Zhai Sheping,Wang Wancheng. "Arch for detecting and tracking of human motion target in video-based sequences",Computer application and software, Vol.23, no.4,2006, pp. 139-141.

[20]Ming-kuei Hu. "Visual Pattern Recognition by Moment Invariants", ROC IRE(Correspondence) Transaction on information theroy, Vol.49, no.1,1962, pp. 179-187.

[21]Liu Xijun, Jia Qifeng. "Theory of engineering vibration and testing technology",Beijing：Higher education press, 2004, pp.390-420.

[22]Ni Zhenhua, "Vibration mechanics",Xi'an : Xi'an jiaotong press,1989, pp. 64-65

[23]Liu Xijun,Jia Qifeng, "Theory of engineering vibration and testing technology", Beijing:Higer education press, 2004, pp. 390-420.